Article

J. Biol. Regul. Homeost. Agents. 2024; 38(7): 5415–5427
https://doi.org/10.23812/j.biol.regul.homeost.agents.20243807.434

Pitavastatin Improves Doxorubicin-Induced Nephrotic Syndrome by Inhibiting the IL-13/p-STAT6 Pathway

Yuanqin Xu[1], Xue Zhang[2], Yan An[3], Yan Chen[4], Meifeng Huo[4], Tao Feng[4,*]

[1]Neurology Department, The Second Affiliated Hospital of Baotou Medical College, Inner Mongolia University of Science and Technology, 014000 Baotou, Inner Mongolia Autonomous Region, China
[2]Ultrasound Room, The Second Affiliated Hospital of Baotou Medical College, Inner Mongolia University of Science and Technology, 014000 Baotou, Inner Mongolia Autonomous Region, China
[3]Rheumatology and Immunology Department, The Second Affiliated Hospital of Baotou Medical College, Inner Mongolia University of Science and Technology, 014000 Baotou, Inner Mongolia Autonomous Region, China
[4]Nephrology Department, The Second Affiliated Hospital of Baotou Medical College, Inner Mongolia University of Science and Technology, 014000 Baotou, Inner Mongolia Autonomous Region, China
*Correspondence: taofeng1623423258@163.com (Tao Feng)
Submitted: 25 March 2024 Revised: 19 April 2024 Accepted: 9 May 2024 Published: 1 July 2024

Background: Doxorubicin (DOX) is a commonly used antineoplastic medication in clinical settings. However, its clinical utility is hampered by pronounced adverse effects such as nephrotoxicity. The interleukin (IL)-13/p-signal transducer and activator of transcription 6 (STAT6) pathway plays a critical role in various renal diseases. Furthermore, Pitavastatin, a statin drug, has been recognized for its protective effects against multiple diseases. Therefore, this study aimed to explore whether Pitavastatin could improve doxorubicin-induced experimental nephrotoxicity by inhibiting the IL-13/p-STAT6 pathway.

Methods: In this study, a doxorubicin-induced mouse model of renal injury was employed, and mice were randomly divided into five groups: the normal control, Pitavastatin, doxorubicin, doxorubicin + dimethyl sulfoxide (DMSO), and doxorubicin + Pitavastatin groups. Their renal function was assessed by observing mouse body weight and serum biochemical markers (urea nitrogen, creatinine, cystatin C). Western blot analysis was used to examine the levels of IL-13 and STAT6, their phosphorylation in renal tissues, and the expression of inflammatory factors. The effects of Pitavastatin on doxorubicin-induced oxidative stress and apoptosis were analyzed through 2,7-dichlorodihydrofluorescein diacetate (DCF-DA) fluorescence staining and terminal deoxynucleotidyl transferase dUTP nick end labeling (TUNEL) staining.

Results: Compared to the doxorubicin group, the doxorubicin + Pitavastatin group showed a significant reduction in mouse body weight and improvement in serum biochemical markers ($p < 0.05$), indicating that Pitavastatin effectively ameliorated doxorubicin-induced nephrotoxicity. Furthermore, Pitavastatin suppressed the IL-13/p-STAT6 pathway's activity and reduced the expression of inflammatory factors at the molecular level. Additionally, Pitavastatin alleviated doxorubicin-induced oxidative stress and apoptosis.

Conclusion: This study demonstrates that Pitavastatin can alleviate doxorubicin-induced nephrotoxicity by inhibiting the IL-13/p-STAT6 pathway. This effect may be correlated to its anti-inflammatory, antioxidant, and anti-apoptotic capabilities. Therefore, Pitavastatin can be a promising therapeutic drug for treating doxorubicin-induced nephrotoxicity. Furthermore, these findings offer a novel theoretical foundation for the therapeutic use of Pitavastatin and suggest future avenues for additional clinical investigations.

Keywords: Pitavastatin; DOX-induced nephrotoxicity; IL-13/p-STAT6 pathway; oxidative stress; renal protection

Introduction

Doxorubicin (DOX), an antineoplastic drug, has been extensively used in treating various cancers due to its remarkable anticancer efficacy [1–3]. However, its clinical application is limited by pronounced adverse effects, such as cardiotoxicity and nephrotoxicity. DOX-induced nephrotoxicity (DOX IN), a prominent adverse impact of DOX, is characterized by glomerular and tubular damage within the kidneys [4–6].

Over the past few years, the interleukin-13 (IL-13)/p-signal transducer and activator of transcription 6 (STAT6) pathway has been extensively studied due to its potential role in various inflammatory and fibrotic diseases [7,8]. IL-13, an immunoregulatory cytokine, participates in regulating inflammatory responses and fibrotic processes through the activation of the STAT6 signaling pathway [9–11]. The activation of IL-13/p-STAT6 in renal disease models is closely associated with the progression of renal inflammation and fibrosis [11,12].

Journal of
BIOLOGICAL REGULATORS
and Homeostatic Agents

Pitavastatin, an the 3-hydroxy-3-methylglutaryl coenzyme-A (HMG-CoA) reductase inhibitor primarily used to lower serum cholesterol levels, has recently been found to possess potential anti-inflammatory, antioxidant, and antifibrotic effects [13–16]. Numerous studies have revealed the significance of the IL-13/p-STAT6 pathway in renal diseases, and the potential anti-inflammatory and antifibrotic effects of Pitavastatin. However, none of the studies has attempted to investigate the preventive or therapeutic impacts of Pitavastatin on DOX-induced nephrotic disease by inhibiting the IL-13/p-STAT6 pathway. Furthermore, the impacts of Pitavastatin on various components of the IL-13/p-STAT6 pathway and the significance of these effects in mitigating kidney damage and promoting renal repair remain unexplored.

Therefore, this study aimed to investigate the therapeutic impacts of Pitavastatin on DOX-induced experimental nephrotoxicity by inhibiting the IL-13/p-STAT6 pathway and to explore its underlying potential mechanisms. Additionally, it was intended to examine the effects of Pitavastatin on renal function, renal inflammatory responses, and fibrosis by establishing an experimental DOX-induced nephrotoxicity model. Furthermore, the regulatory impact of Pitavastatin on the IL-13/p-STAT6 pathway was also evaluated. This study provides significant insights into developing novel treatment strategies for DOX IN and offers a theoretical foundation for utilizing Pitavastatin in treating other inflammatory and fibrotic diseases.

Materials and Methods

DOX-Induced Nephrotic Syndrome Mouse Model

Thirty male SPF-grade BALB/c mice (aged 8 weeks and weighing 25~30 grams) were purchased from Zhejiang Vital River Laboratory Animal Technology Co., Ltd., Jiaxing, China with the license number SYXK (Su) 2018-0020. The mice were housed in a barrier facility with free access to food and water. The temperature and humidity were maintained at 20~26 °C and 40%~70%, respectively, with a 12 h light/dark cycle. The experimental protocols involving animals were approved by the Animal Ethics Committee of The Second Affiliated Hospital of Baotou Medical College, Inner Mongolia University of Science and Technology (LW-005). DOX was obtained from MedChemExpress (HY-15142A). After a week of acclimatization, the mice were randomly classified into five groups: the Normal, Pitavastatin, DOX, DOX + dimethyl sulfoxide (DMSO), and DOX + Pitavastatin groups, each group comprising 6 mice. The Normal group received an intravenous injection of PBS, whereas the model groups received an intravenous injection of DOX (5 mg/kg). Additionally, the DOX + Pitavastatin group received a concurrent intraperitoneal injection of Pitavastatin (10 mg/kg). Furthermore, urine samples were collected every 24 hours using metabolic cages over two weeks. Subsequently, the mice were euthanized through cervical dislocation followed by harvesting kidney tissues and collecting blood samples for further experimentation.

Biochemical Analysis

The urine samples from the mice were collected to assess 24-hour urinary protein (UP) levels. After this, the mice were euthanized by injecting pentobarbital sodium (21642-83-1, Shandong Xiya Chemical Industry Co., Ltd., Linshu, China, 2%, 40 mg/kg) intraperitoneally, and blood samples were collected from their abdominal aorta. The blood samples were centrifuged to isolate serum to evaluate the serum cystatin C (CYS-C), serum creatinine (Scr), and blood urea nitrogen (BUN) levels. The 24-hour UP levels were detected using the bicinchoninic acid (BCA, A045-4-2, Nanjing Jiancheng Bioengineering Institute, Nanjing, China) method, whereas Scr, BUN, and CYS-C were measured using an automatic biochemical analyzer (AU5800, Beckman Coulter, Brea, CA, USA).

Enzyme-Linked Immunosorbent Assay (ELISA)

The corresponding ELISA kits for interleukin (IL)-1β (Cat No. EK201B), IL-6 (Cat No. EK206), and tumor necrosis factor (TNF)-α (Cat No. EK282) were purchased from Hangzhou Lianke Biotech Co., Ltd., Hangzhou, China and their expression levels in serum and HK-2 cells were determined following the protocols provided with the kits. ROS ELISA kit (S0033S), malondialdehyde (MDA) ELISA kit (S0131S), and lactate dehydrogenase (LDH) ELISA kit (C0016) were used to assess cellular oxidative stress and damage. These kits were obtained from Beyotime, Shanghai, China. The experimental results obtained from these assays were normalized.

Western Blot

Animal Protein Extraction

Initially, mouse kidney tissues were homogenized using a tissue grinder, followed by adding Radio Immunoprecipitation Assay Lysis (RIPA, W062-1-1, Nanjing Jiancheng Bioengineering Institute, Nanjing, China) buffer and protease inhibitor phenylmethanesulfonyl fluoride (PMSF, P0100, Solarbio Life Sciences, Beijing, China). The mixture was then lysed on ice and the lysate was centrifuged (11,296 g) at 4 °C for 30 minutes. The resultant supernatant was utilized to quantify protein content through the BCA technique. Finally, the protein lysate was stored at –80 °C for further analysis.

Cell Protein Extraction

After experimental treatment, the culture medium was discarded and the cells were washed with PBS and lysed on ice using RIPA lysis buffer and protease inhibitor. The cells were scraped from the culture dish, and transferred to 1.5 mL EP tubes. The cell lysate was centrifuged, and the proteins were quantified using the BCA tech-

nique. For each group, 25 μg of the quantified proteins were loaded onto a gel for separation using 12% Sodium dodecyl sulfate polyacrylamide gel electrophoresis (SDS-PAGE) (89888, Thermo Fisher Scientific, Waltham, MA, USA) and then transferred to the polyvinylidene difluoride (PVDF) membrane (88585, Thermo Fisher Scientific, Waltham, MA, USA). After this, the membranes were blocked with 5% skim milk for 2 hours. The membranes were incubated overnight with primary antibodies (diluted at 1:1000) against IL-13 (#DF6813, Affinity, Liyang, China), p-STAT6 (Tyr641) (#AF3301, Affinity, Liyang, China), STAT6 (#AF6302, Affinity, Liyang, China), Bax (#2772, CST, BSN, MA, USA), Bcl-2 (#15071, CST, BSN, MA, USA), and glyceraldehyde-3-phosphate dehydrogenase (GAPDH, #2118, CST, BSN, MA, USA) at 4 °C. The following day, the membranes were incubated with secondary antibody for one hour at room temperature. After washing with TBST, the blots were developed and visualized using a chemiluminescence enhanced chemiluminescence (ECL) reagent (BL520B, Biosharp Life Sciences, Hefei, China). The gray value of strip was analyzed using ImageJ software (v1.8.0.345, National Institutes of Health, Bethesda, MD, USA), and GAPDH was used as the internal control for quantifying the expression of target proteins.

HK-2 and NRK-52E Cell Culture

Human proximal tubular epithelial cells (HK-2, CRL-2190) and rat epithelial cell line NRK-52E (CRL-1571) were obtained from the American Type Culture Collection (ATCC, Manassas, VA, USA). The cells were validated using short tandem repeat (STR) analysis and were screened for cross-contamination using mycoplasma testing. The experimental procedures followed the protocols outlined by You *et al*. [17], Cheng *et al*. [18], Ni *et al*. [19], and Long *et al*. [20], with slight modifications. HK-2 and NRK-52E cells were cultured in RPMI-1640 medium (KeyGEN BioTECH, Nanjing, China) supplemented with 10% fetal bovine serum (FBS) (Gibco, New York, NY, USA) and incubated at 37 °C and 5% CO_2 to promote cell proliferation. The culture medium was refreshed with pre-warmed medium every 1–2 days. The cells were categorized into 5 groups, such as the control group, the DOX (5 μM) group, the DOX + DMSO group, the DOX + Pitavastatin (10 μM) group, and the DOX + Pitavastatin + IL-13 (10 ng/mL) group. The cells underwent an additional 24-hour incubation before being proceeded for subsequent experiments.

Cell Counting Kit-8 (CCK-8) Assay

The cell viability was assessed using a Cell Counting Kit-8 (CCK-8) (Dojindo Laboratories, Kumamoto, Japan). To perform this, cells in the logarithmic growth phase were adjusted to an appropriate concentration and seeded into a 96-well plate with a density of 2.5×10^3 cells per well. After 24 hours of incubation to facilitate cell attachment, the cells were treated with DOX (5 μM), Pitavastatin (10 μM), and IL-13 (10 ng/mL) and allowed to incubate for another 48 hours at 37 °C and 5% CO_2. Subsequently, 10 μL of CCK-8 reagent was added to each well and incubated for an additional hour. The OD was measured using a microplate reader, and the inhibition rate of cell proliferation was determined. The experiments were replicated three times to ensure reproducibility and accuracy.

5-Ethynyl-2′-Deoxyuridine (EdU) Assay for Cell Proliferation

Cells, administered with experimental treatment, were cultured onto coverslips within a 6-well plate at a density of 1×10^5 cells per well and incubated with EdU solution at a concentration of 10 μmol/L for 2 hours. The cells were then permeabilized for 10 minutes using 0.5% Triton X-100, fixed for 15 minutes at room temperature with 4% paraformaldehyde, and stained for 30 minutes with 4′,6-diamidino-2-phenylindole (DAPI). After phosphate buffer saline (PBS) washing and glycerol sealing, microscopy was performed using a fluorescence microscope (CX41-32RFL, Olympus Corporation, Tokyo, Japan). The presence of blue fluorescence signifies the nuclei of cells, while red fluorescence marks the cells that are EdU-positive. To enumerate the population of total and EdU-positive cells, six visual fields were randomly selected. The rate of EdU incorporation was determined using the formula: EdU positive rate (%) = (EdU-positive cell count/Total cell count) × 100%.

Reactive Oxygen Species (ROS) Detection Using DCFH-DA Assay

To detect ROS levels using 2′,7′-dichlorodihydrofluorescein diacetate (DCFH-DA) assay, 1 mL of HK-2 cell suspension containing 5×10^4 cells was cultured in a 35 mm confocal dish. After achieving 90% confluence, the cells were treated for 24 hours. Subsequently, 1 mL of PBS containing the DCFH-DA probe was added to the cells and incubated at room temperature for 30 minutes. Finally, the cells were observed using a laser confocal microscope (Excitation wavelength: 488 nm and Emission wavelength: 525 nm), and photographs were captured.

Terminal Deoxynucleotidyl Transferase dUTP Nick End Labeling (TUNEL) Staining for Apoptosis Detection

HK-2 and NRK-52E cells were seeded separately in 12-well plates and subsequently treated with 0.1% Triton X-100 (BL934B, Biosharp, Anhui, China) to facilitate permeabilization. Following this, the cells were treated with 200 μL of 3% H_2O_2 (H6520, Merck, Darmstadt, Germany) and subsequently rinsed with PBS before applying proteinase K to deactivate any enzymes in the cells. The cells were incubated with the TUNEL reagent (40306ES60, Yeasen, Shanghai, China) in the dark for 60 minutes followed by three PBS washes. Subsequently, the cells were stained us-

Journal of
BIOLOGICAL REGULATORS
and Homeostatic Agents

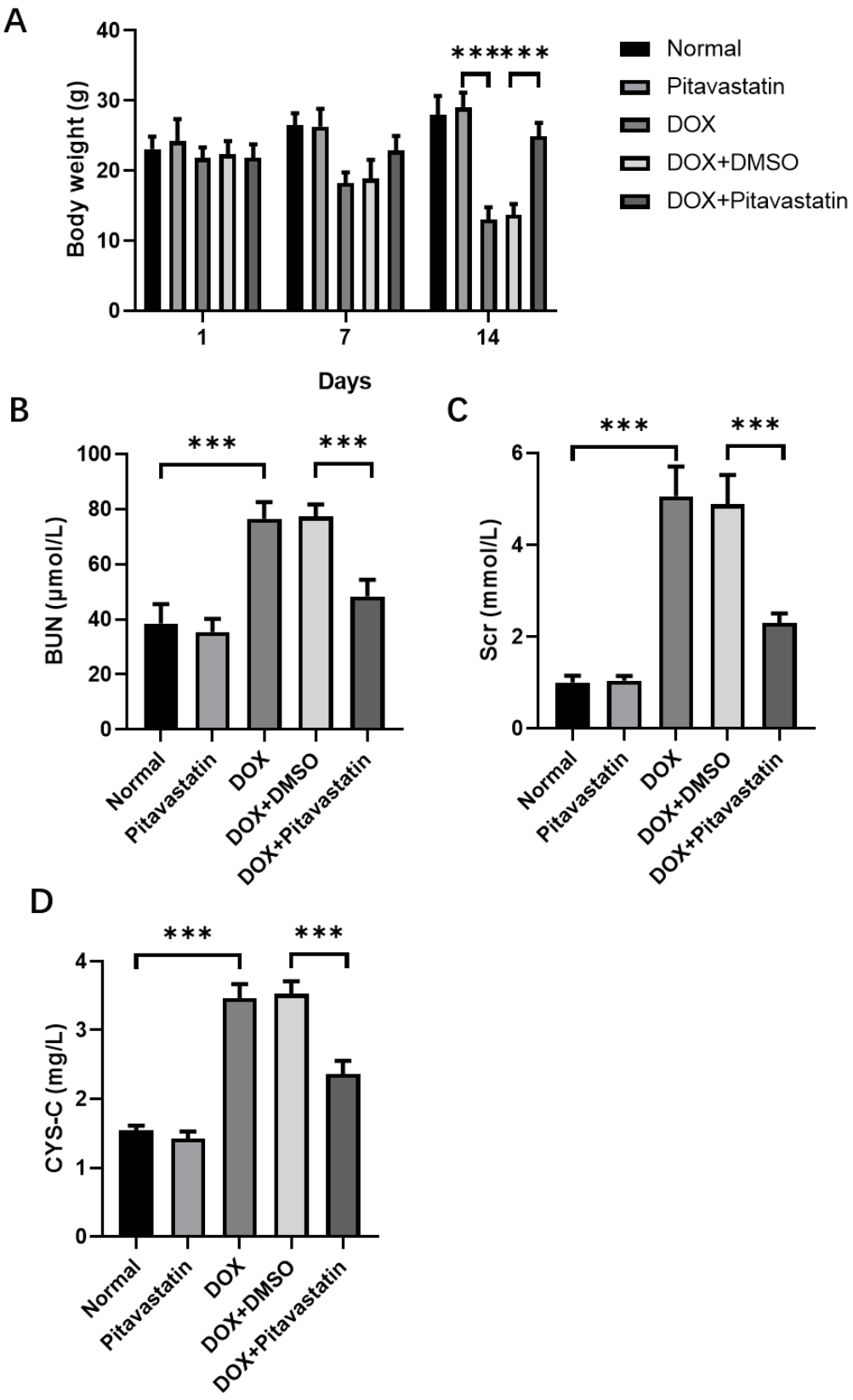

Fig. 1. DOX-induced weight loss and serum biochemical parameter changes in mice. (A) The body weight of mice was measured during the experimental period (days 1, 7, and 14). $^{***}p < 0.001$. (B–D) Levels of BUN (B), Scr (C), and CYS-C (D) in serum from mice of different treatment groups. $^{***}p < 0.001$. Abbreviations in the figure are as follows: BUN, blood urea nitrogen; Scr, serum creatinine; CYS-C, serum cystatin C; DOX, doxorubicin; DMSO, dimethyl sulfoxide.

ing a DAPI solution (40728ES, Yeasen, Shanghai, China) for twenty minutes and sealed to observe using fluorescence microscopy. Apoptotic cells were visualized using green fluorescence, whereas live cells were examined using blue fluorescence. The percentage of apoptotic cells was determined using the formula: Apoptosis rate = (Count of apoptotic cells per field/Total cell count per field) $\times$ 100%.

Statistical Analysis

Statistical analysis was conducted using the GraphPad Prism 8 software (GraphPad Software, Inc., San Diego, CA, USA) package and IBM SPSS statistical software 26 (IBM Corp., Armonk, NY, USA). The quantitative data were presented in the form of mean $\pm$ standard deviation. Two distinct groups were compared using the *t*-test, whereas multiple groups were compared using one-way analysis of variance (ANOVA) followed by Duncan multiple range tests. A *p*-value less than 0.05 was considered statistically significant.

Results

DOX-Induced Weight Loss and Changes in Serum Biochemical Parameters in Mice

To explore the effects of Pitavastatin on DOX-induced renal injury, initially, changes in mouse weight and serum biochemical parameters were observed. The findings demonstrated that the body weights of mice in the normal control and those treated with Pitavastatin alone were constant, suggesting that Pitavastatin does not significantly alter body weight. However, the body weights of mice treated with DOX were significantly decreased, indicating the toxic effects of DOX. Furthermore, the weight loss in the DOX + Pitavastatin group was less than that in the DOX group, suggesting that Pitavastatin can mitigate the toxic effects of DOX (Fig. 1A). Blood urea nitrogen (BUN) is an important indicator of kidney function, reflecting the kidney's ability to excrete waste. An increase in the BUN levels indicates kidney damage or impaired function. The BUN levels in the normal control group were significantly lower ($p < 0.001$) compared to the DOX group, indicating that DOX is potentially associated with kidney impairment. Although the BUN levels in the DOX + Pitavastatin group were higher compared to the normal control, they were substantially lower compared to the DOX group ($p < 0.001$), suggesting a crucial role of Pitavastatin in alleviating DOX-induced kidney damage (Fig. 1B).

Serum creatinine levels are used as a biomarker in evaluating kidney filtration performance, where a rise in the levels of this biomarker is a sensitive sign of deterioration in renal function. The pattern of creatinine changes was comparable to that of BUN. Compared to the normal control group, the creatinine levels were significantly higher in the DOX group ($p < 0.001$), indicating kidney damage. Furthermore, the creatinine levels in the DOX + Pitavastatin group were higher than those in the control group, while significantly lower than in the DOX group. These observations further validate the protective effects of Pitavastatin on DOX-induced kidney injury (Fig. 1C). The results for cystatin C were consistent with those of BUN and creatinine, further validating the protective effects of Pitavastatin on DOX-induced kidney injury (Fig. 1D).

Pitavastatin Inhibited the IL-13/p-STAT6 Pathway in Renal Tissue and Reduced Serum Inflammatory Cytokines Levels

IL-13, a cytokine primarily produced by Th2 cells, can promote inflammation and fibrosis, and its overexpression is associated with various inflammatory diseases [21]. The phosphorylated form of STAT6 plays a crucial role in activating the IL-13 signaling pathway, thereby regulating inflammation [22]. Compared to the normal group, DOX treatment significantly increased the expression levels of IL-13 and p-STAT6 ($p < 0.001$), indicating DOX-induced activation of the IL-13/p-STAT6 pathway, contributing to inflammation in kidney injury. Furthermore, DOX-induced activation of the IL-13/p-STAT6 pathway was effectively impeded following Pitavastatin treatment (Fig. 2A–C). Moreover, compared to the normal group, DOX treatment significantly elevated the expression levels of tumor necrosis factor (TNF)-α, interleukin (IL)-1β, and IL-6, which are associated with the exacerbation of kidney injury and inflammatory response. However, Pitavastatin treatment reduced these inflammatory cytokines, indicating its anti-inflammatory effects and its potential to alleviate DOX-induced kidney injury (Fig. 2D–F).

Protective Effects of Pitavastatin on HK-2 and NRK-52E Cell Viability Following DOX Treatment

We evaluated the protective effects of Pitavastatin on HK-2 and NRK-52E cell viability after DOX treatment. Both CCK-8 and EdU assays demonstrated that cell viability was the highest in the control group (Ctrl), indicating that under normal conditions without DOX treatment, HK-2 cells exhibited the strongest activity and proliferation capability. Furthermore, compared to both the DOX treatment group (DOX) and the DOX + DMSO group, the cell viability was significantly higher in the Pitavastatin treatment group (DOX + Pitavastatin) ($p < 0.001$), indicating that Pitavastatin improved the reduction in cell viability induced by DOX, exerting protective effects (Fig. 3A,B). Cell viability in the DOX-treated group and the DOX + DMSO group demonstrated comparable and lower than the Pitavastatin treatment group, indicating that DOX inhibited cell viability, while DMSO did not confer protection.

Similarly, CCK-8 and EdU assay indicated that NRK-52E cell viability was the highest in the control group ($p < 0.001$). Compared to both the DOX-treated group and the DOX + DMSO group, the Pitavastatin-treated group ex-

Journal of
BIOLOGICAL REGULATORS
and Homeostatic Agents

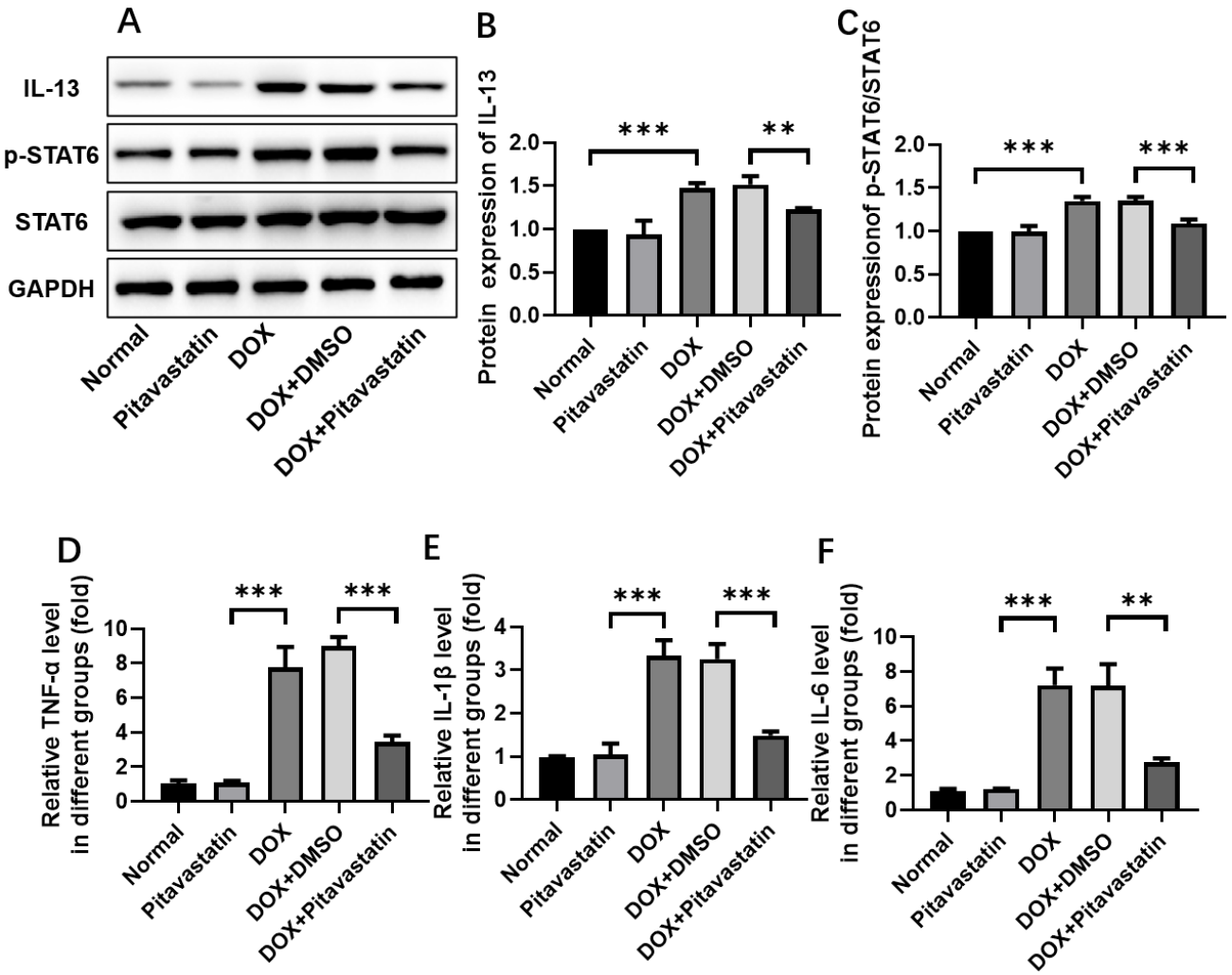

Fig. 2. Pitavastatin inhibited the interleukin (IL)-13/p-signal transducer and activator of transcription 6 (STAT6) pathway in renal tissues and alleviated the levels of inflammatory cytokines in serum. (A–C) The expression levels of IL-13, phosphorylated (p)-STAT6, and total (t)-STAT6 were determined in the renal tissues of treated groups using Western blot analysis. (D–F) Serum levels of tumor necrosis factor (TNF)-α (D), interleukin (IL)-1β (E), and IL-6 (F) were evaluated using enzyme-linked immunosorbent assay (ELISA). $^{**}p < 0.01$, $^{***}p < 0.001$. GAPDH, glyceraldehyde-3-phosphate dehydrogenase; DMSO, dimethyl sulfoxide.

hibited significantly higher cell viability ($p < 0.05$). These findings indicate that Pitavastatin protects NRK-52E cells from DOX-induced damage (Fig. 3C,D).

Effects of Pitavastatin on IL-13/p-STAT6 Signaling and Inflammation in HK-2 Cells, with IL-13 Exacerbating Inflammatory Damage

We investigated the specific effects of Pitavastatin on IL-13/p-STAT6 signaling and inflammation in HK-2 cells, along with how IL-13 exacerbates inflammatory damage. The DOX therapy substantially increased the expression levels of p-STAT6 and IL-13 ($p < 0.001$). Treatment with Pitavastatin (DOX + Pitavastatin group) significantly reduced the expressions of IL-13 and p-STAT6 ($p < 0.01$), demonstrating that Pitavastatin can inhibit the activation of the IL-13/p-STAT6 pathway induced by DOX. However, the addition of IL-13 (DOX + Pitavastatin + IL-13 group) again significantly increased the expressions of IL-13 and p-STAT6 ($p < 0.01$), suggesting that exogenous IL-13 can reverse the inhibitory effect of Pitavastatin (Fig. 4A–C). Similar to the trend in IL-13 and p-STAT6 expressions, DOX treatment significantly increased the levels of these inflammatory cytokines, while Pitavastatin treatment substantially reduced their levels ($p < 0.001$). This finding indicates that Pitavastatin can alleviate the inflammatory response induced by DOX. After the addition of IL-13, the levels of these inflammatory cytokines increased again ($p < 0.01$), further validating the role of IL-13 in the inflammatory response and affirming the anti-inflammatory property of Pitavastatin through the inhibition of the IL-13/p-STAT6 pathway (Fig. 4D–F).

The findings from the EdU assay showed that DOX treatment significantly reduced the proliferative capacity of HK-2 cells ($p < 0.001$), whereas Pitavastatin treatment

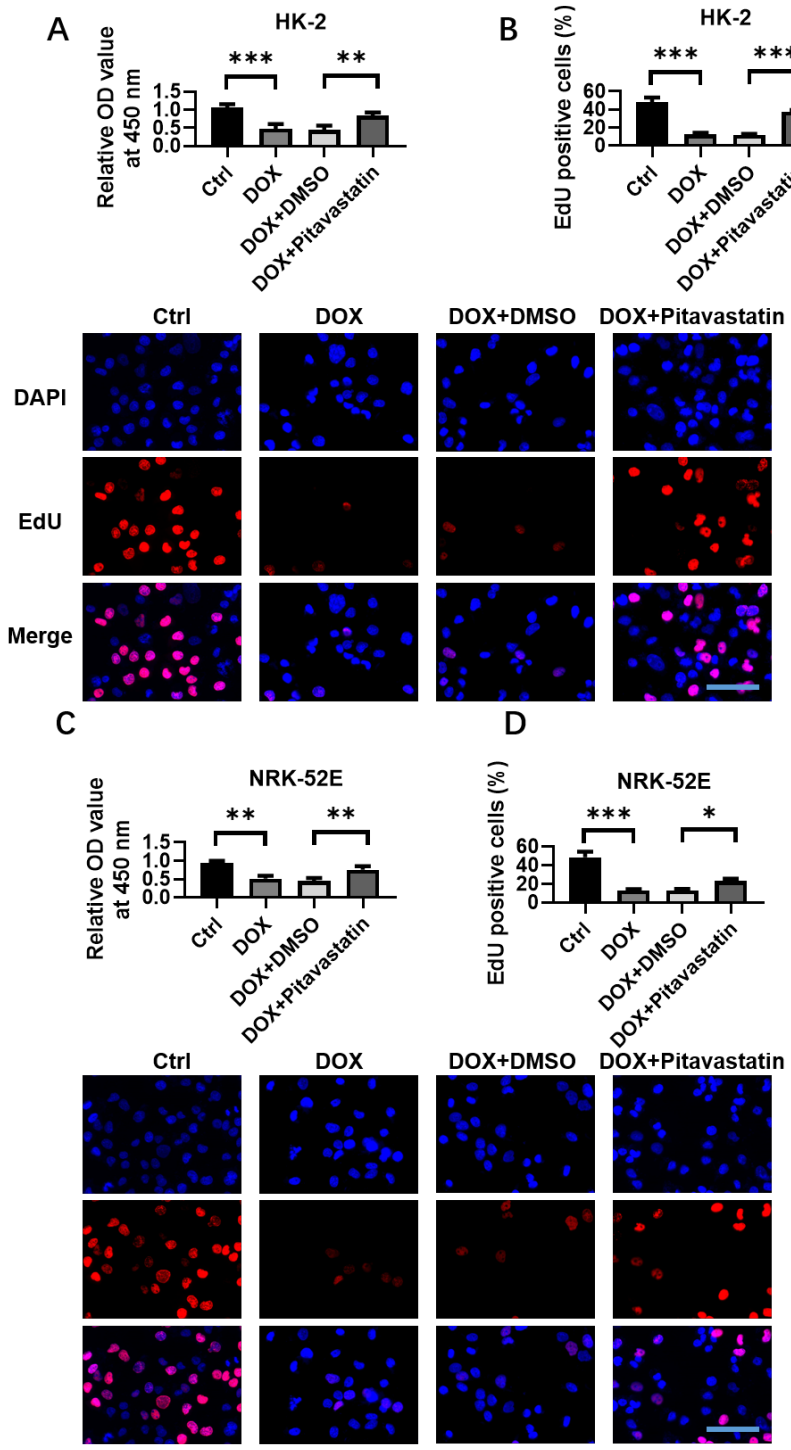

Fig. 3. Protective effect of Pitavastatin on HK-2 and NRK-52E cell viability following doxorubicin treatment. (A) CCK-8 assay was used to evaluate the protective effect of Pitavastatin on HK-2 cell viability. (B) EdU assay was utilized to assess the protective effect of Pitavastatin on HK-2 cell viability. (C) CCK-8 assay was used to evaluate the protective effect of Pitavastatin on NRK-52E cell viability. (D) EdU assay was employed to assess the protective effect of Pitavastatin on NRK-52E cell viability. Scale bar: 100 μm. $^{*}p < 0.05$, $^{**}p < 0.01$, $^{***}p < 0.001$. DAPI, 4′,6-diamidino-2-phenylindole; EdU, 5-ethynyl-2′-deoxyuridine; CCK-8, Cell Counting Kit-8.

improved cell proliferation, indicating its protective effect against DOX-induced cellular damage. However, after the addition of IL-13, there was no significant improvement in cell proliferation, which may be due to IL-13 exacerbating inflammatory damage, thus offsetting the protective effect of Pitavastatin (Fig. 4G).

Journal of
BIOLOGICAL REGULATORS
and Homeostatic Agents

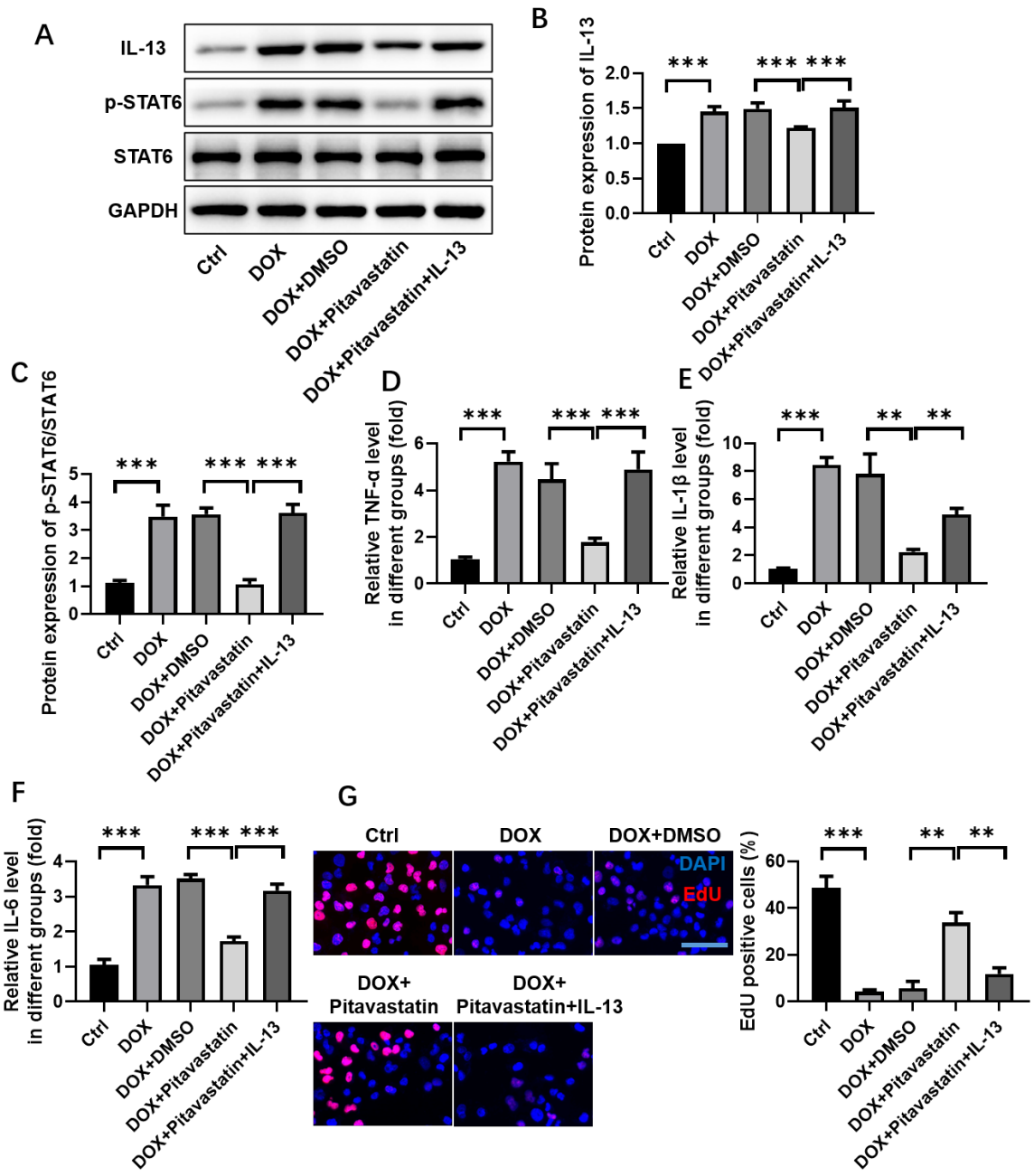

Fig. 4. Effects of Pitavastatin on IL-13/p-STAT6 signaling and inflammation in HK-2 cells, with IL-13 treatment exacerbating inflammatory damage. (A–C) The expression levels of IL-13, p-STAT6, and STAT6 were assessed in different groups using Western blot analysis. (D–F) Levels of TNF-α (D), IL-1β (E), and IL-6 (F) in cells. (G) The protective effect of Pitavastatin on HK-2 cell viability was evaluated utilizing EdU assay. Scale bar: 100 µm. $^{**}p < 0.01$, $^{***}p < 0.001$.

Pitavastatin Inhibited Oxidative Stress, Exerting Protective Effects on HK-2 Cells

We elucidated how Pitavastatin exerts protective effects on HK-2 cells by inhibiting oxidative stress. We observed the potential antioxidative role of Pitavastatin. The control group showed the lowest reactive oxygen species (ROS), malondialdehyde (MDA), and lactate dehydrogenase (LDH) levels, indicating reduced oxidative stress and damage under normal conditions ($p < 0.001$). Conversely, DOX treatment (DOX and DOX + DMSO groups) resulted in a significant increase in ROS, MDA, and LDH levels ($p < 0.01$), suggesting significant oxidative stress and cellular damage induced by DOX. Furthermore, Pitavastatin treatment (DOX + Pitavastatin group) significantly reduced ROS, MDA, and LDH levels ($p < 0.05$). However, after the addition of IL-13 (DOX + Pitavastatin + IL-13 group), ROS, MDA, and LDH were comparable to those in the DOX treatment group, indicating that IL-13 can reverse the protective effect of Pitavastatin (Fig. 5A–C).

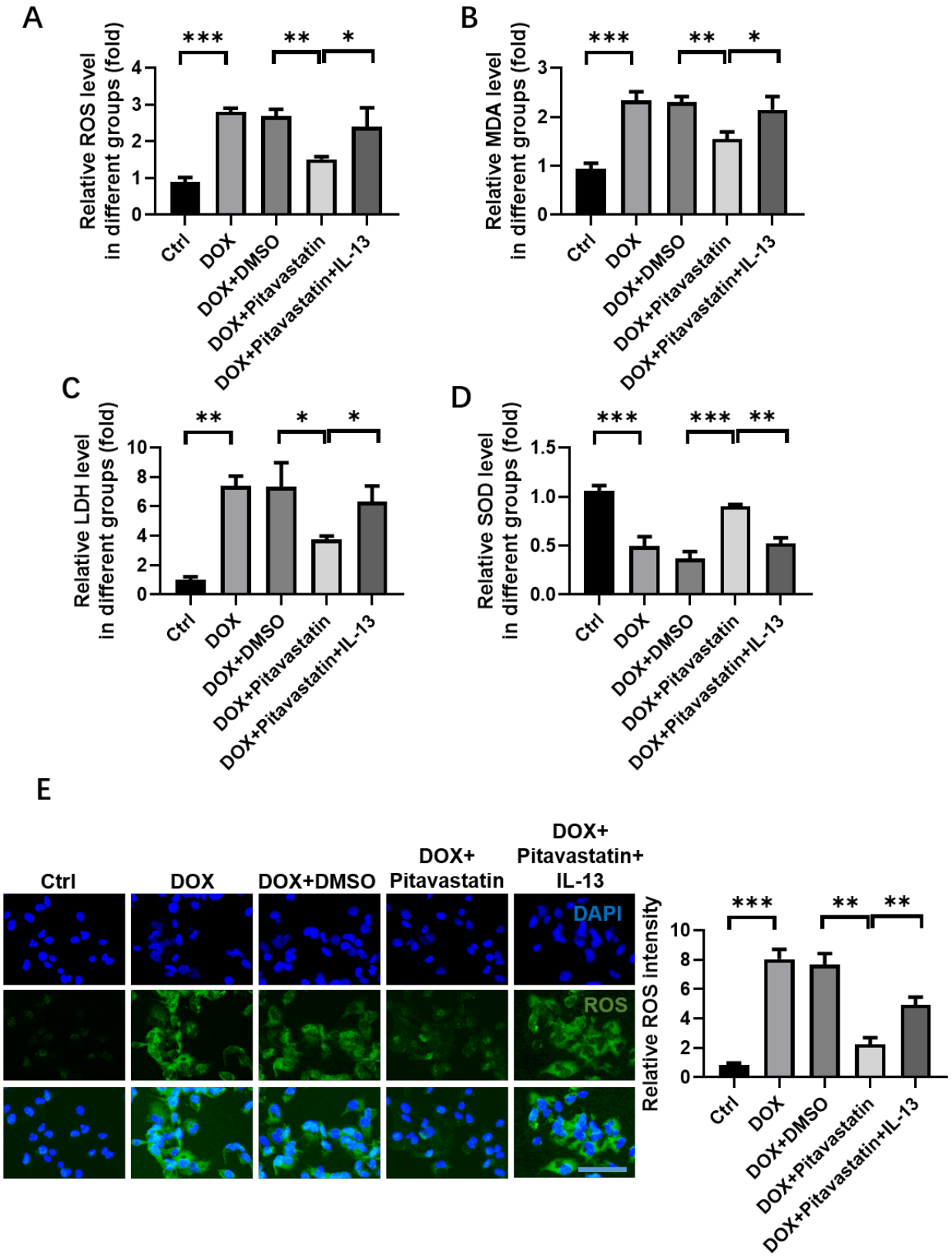

Fig. 5. Pitavastatin mitigated oxidative stress and exerted protective effects on HK-2 cells. (A–C) The levels of ROS (A), MDA (B), and LDH (C) were assessed using ELISA. (D) The levels of superoxide dismutase (SOD) were evaluated in different treatment groups using ELISA. (E) ROS activity was observed by measuring DCF-DA fluorescence intensity under fluorescence microscopy. Scale bar: 50 μm. $^{*}p < 0.05$, $^{**}p < 0.01$, $^{***}p < 0.001$. Abbreviations in the figure are as follows: ROX, reactive oxygen species; MDA, malondialdehyde; LDH, lactate dehydrogenase.

Journal of
BIOLOGICAL REGULATORS
and Homeostatic Agents

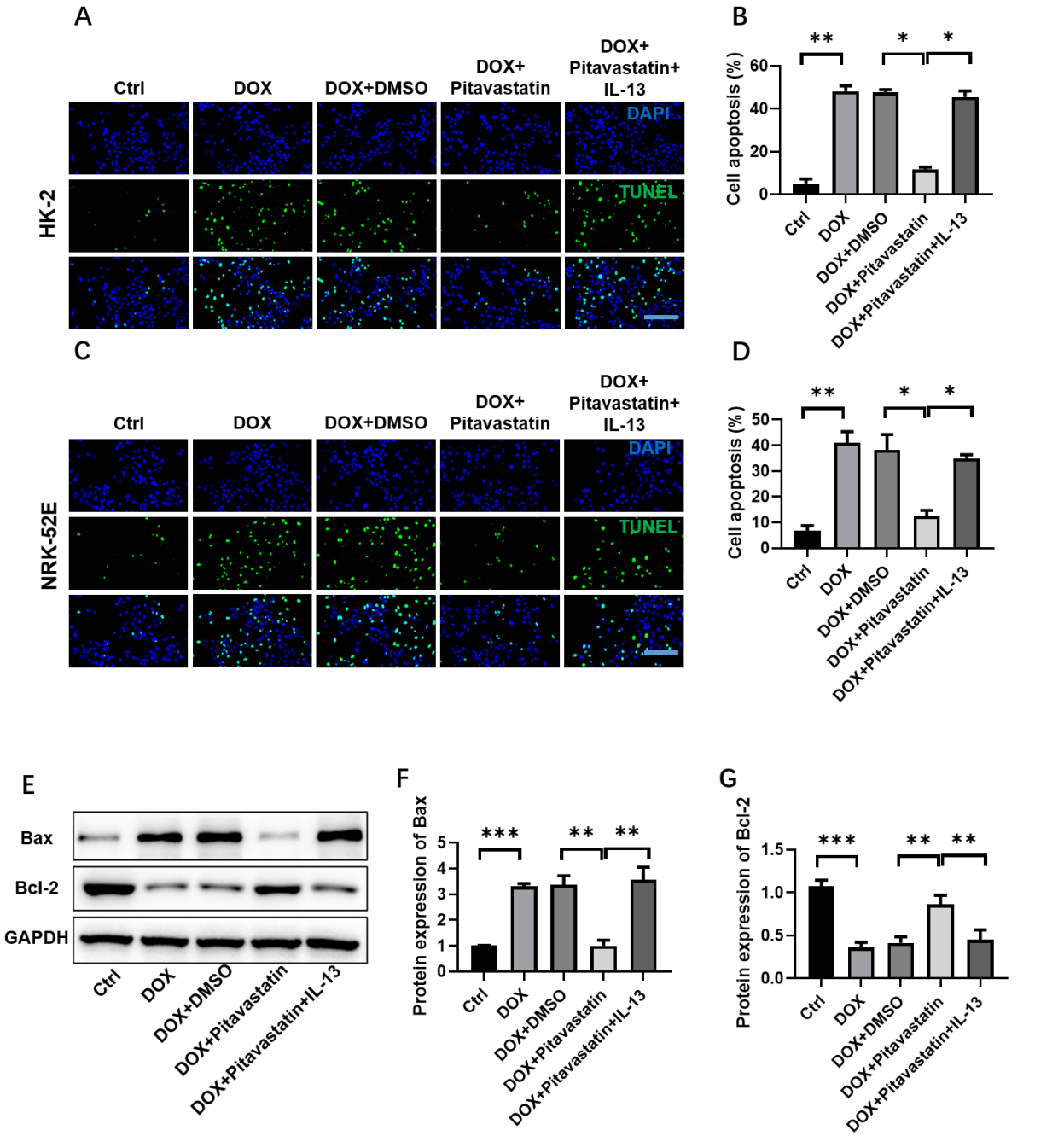

Fig. 6. Effects of Pitavastatin on apoptosis in HK-2 and NRK-52E cells following doxorubicin treatment. (A) Apoptosis in HK-2 cells was assessed using TUNEL staining after different treatments. (B) Statistical analysis of apoptosis in each group. (C) Apoptosis in NRK-52E cells was assessed through TUNEL staining after different treatments. (D) Statistical analysis of apoptosis. (E–G) Western blot analysis of apoptosis markers (Bax, Bcl-2-associated X protein; Bcl-2, B-cell lymphoma-2) in cells following doxorubicin treatment. Scale bar: 200 μm. $^{*}p < 0.05$, $^{**}p < 0.01$, $^{***}p < 0.001$. TUNEL, terminal deoxynucleotidyl transferase dUTP nick end labeling.

The superoxide dismutase (SOD) activity results showed that the control group exhibited the highest SOD activity ($p < 0.001$), suggesting robust antioxidative capabilities. In contrast, DOX treatment significantly reduced SOD activity ($p < 0.001$), indicating that DOX impaired the cell's antioxidative defense mechanism. Moreover, Pitavastatin treatment significantly increased SOD activity ($p < 0.001$), demonstrating its ability to enhance the cell's antioxidative capacity and alleviate oxidative stress. However, after the addition of IL-13, SOD activity was comparable to the DOX treatment group, indicating that IL-13 negated the antioxidative effect of Pitavastatin (Fig. 5D). The control group showed the lowest DCF-DA fluorescence intensity, suggesting lower ROS activity. DOX treatment significantly increased DCF-DA fluorescence intensity ($p < 0.001$), indicating increased ROS production. In contrast,

Pitavastatin treatment resulted in a significant reduction in DCF-DA fluorescence intensity ($p < 0.01$), demonstrating its ability to reduce ROS production and alleviate oxidative stress. However, after the addition of IL-13, DCF-DA fluorescence intensity was comparable to the DOX treatment group, further validating that IL-13 can reverse the antioxidative protective effect of Pitavastatin (Fig. 5E).

Effects of Pitavastatin on HK-2 and NRK-52E Cells Apoptosis after DOX Treatment

Finally, we examined the effects of Pitavastatin on HK-2 and NRK-52E cells apoptosis following DOX treatment. Analysis involving HK-2 cells revealed that the apoptosis rate was significantly reduced in the control group ($p < 0.01$). In contrast, the DOX treatment group (DOX and DOX + DMSO) and the DOX + Pitavastatin + IL-13 group showed comparable and increased cell apoptosis rates, indicating the induction of apoptosis by DOX. However, the addition of IL-13 reversed the protective effect of Pitavastatin. Notably, the Pitavastatin treatment group (DOX + Pitavastatin) showed a higher apoptosis rate than the control group. However, it was significantly lower than that of the DOX treatment group ($p < 0.05$), indicating that Pitavastatin can reduce DOX-induced cell apoptosis (Fig. 6A,B).

Furthermore, analysis involving NRK-52E cells demonstrated that the control group exhibited the lowest cell apoptosis rate. Conversely, the DOX treatment group (DOX and DOX + DMSO) and the DOX + Pitavastatin + IL-13 group showed comparable and increased cell apoptosis rate. The Pitavastatin treatment group (DOX + Pitavastatin) exhibited a higher apoptosis rate than the control group, although it was significantly lower than the DOX treatment group ($p < 0.001$). Moreover, we observed that Pivastatin alleviated DOX-induced apoptosis (Fig. 6C,D).

The expression analysis of Bax and Bcl-2 proteins revealed that the control group exhibited the lowest Bax expression ($p < 0.001$). In contrast, the DOX treatment group and the DOX + Pitavastatin + IL-13 group showed the highest and equal levels of Bax expression ($p < 0.01$). The Pitavastatin treatment group exhibited lower Bax expression than the DOX treatment group ($p < 0.01$), indicating that Pitavastatin can reduce Bax expression, thereby reducing cell apoptosis. Moreover, the control group showed the highest expression of Bcl-2 ($p < 0.001$), while the DOX treatment group and the DOX + Pitavastatin + IL-13 group exhibited the lowest and equal levels of Bcl-2 expression ($p < 0.01$). The Bcl-2 expression levels were significantly higher in the Pitavastatin treatment group than the DOX treatment group but were lower than the control group ($p < 0.01$), indicating that Pitavastatin can increase Bcl-2 expression, thereby inhibiting cell apoptosis (Fig. 6E–G).

Discussion

Previous studies have correlated DOX-induced renal injury with a significant increase in serum biochemical markers [23–25]. Our findings demonstrated that mice treated with Pitavastatin exhibited substantial improvements in renal function indicators compared to the DOX group, suggesting its potential to protect the kidneys from DOX-induced damage. At the molecular level, we found a reduction in the expression levels of IL-13 and phosphorylated STAT6 in renal tissues of mice treated with DOX following Pitavastatin treatment, consistent with previous research. These observations suggest that Pitavastatin acts by inhibiting the IL-13/p-STAT6 pathway. Additionally, Pitavastatin reduced the expression of inflammatory cytokines, further confirming its anti-inflammatory effect [26,27]. Furthermore, studies have shown that Pitavastatin improved cardiac function through the phosphoinositide 3-kinase (PI3K)-protein kinase B (AkT) signaling pathway and protected the liver through the nuclear factor kappa-B (NF-κB) signaling pathway [14,28]. These studies provide the direction for our subsequent investigations.

Related studies have highlighted that DOX-induced renal injury is accompanied by an increase in oxidative stress and apoptosis [29–31]. Notably, the protective effect of Pitavastatin against DOX-induced renal injury is closely related to its inhibition of oxidative stress. Our findings revealed that Pitavastatin reduced ROS and MDA levels while increasing SOD activity, indicating its antioxidant effects. Since oxidative stress is one of the crucial mechanisms of DOX-induced renal injury [29,32], Pitavastatin further protects the kidneys from DOX damage by alleviating oxidative stress. Additionally, we found that Pitavastatin reduced DOX-induced renal cell apoptosis. Through TUNEL staining and Western blot analysis, we observed a reduction in the expression of Bax and an increase in the expression of Bcl-2 after Pitavastatin treatment, indicating that Pitavastatin can inhibit cell apoptosis, thereby protecting renal cells.

This study showed that Pitavastatin effectively inhibits the IL-13/p-STAT6 pathway, thereby ameliorating DOX-induced experimental kidney damage. This finding provides a new perspective for understanding the renal protective mechanism of Pitavastatin and establishes a theoretical foundation for developing new strategies for treating DOX-induced renal injury. Future research should explore the potential efficacy and safety profile of Pitavastatin for clinical use in treating DOX-induced renal injury.

However, this study also has some limitations. The inhibitory mechanism of Pitavastatin on the IL-13/p-STAT6 pathway has not been fully elucidated, requiring further molecular biological research. Moreover, considering that Pitavastatin may potentially modulate other signaling pathways, future studies should explore the effects of Pitavastatin on other related signaling pathways.

Journal of BIOLOGICAL REGULATORS and Homeostatic Agents

Conclusion

In this study, we determine the expression levels of body weight, serum biochemical indexes, and inflammatory factors in DOX-induced mice, validating the beneficial impact of Pitavastatin. Furthermore, Pitavastatin can reduce oxidative stress and apoptosis induced by DOX, thereby protecting renal cells from damage. More importantly, Pitavastatin can mitigate DOX-induced nephrotoxicity by inhibiting the IL-13/p-STAT6 pathway. In summary, this study provides a new perspective on the renal protective mechanism of Pitavastatin, and offers a theoretical basis for the treatment strategy of DOX-induced kidney injury.

Availability of Data and Materials

All experimental data included in this study can be obtained by contacting the first author if needed.

Author Contributions

YQX, YA and YC designed the study; XZ, TF and MFH collected and analyzed the data, YA and TF participated in drafting the manuscript, and all authors contributed to critical revision of the manuscript for important intellectual content. All authors conducted the study. All authors gave final approval of the version to be published. All authors participated fully in the work, took public responsibility for appropriate portions of the content, and agreed to be accountable for all aspects of the work in ensuring that questions related to the accuracy or completeness of any part of the work were appropriately investigated and resolved.

Ethics Approval and Consent to Participate

This study has been approved by the ethics committee of The Second Affiliated Hospital of Baotou Medical College, Inner Mongolia University of Science and Technology, Approval No. LW-005.

Acknowledgment

Not applicable.

Funding

This research was funded by Baotou City Health Science and Technology Plan Project, grant No. wsjkkj024.

Conflict of Interest

The authors declare no conflict of interest.

References

[1] Cappetta D, Rossi F, Piegari E, Quaini F, Berrino L, Urbanek K, *et al*. Doxorubicin targets multiple players: A new view of an old problem. Pharmacological Research. 2018; 127: 4–14.

[2] van der Zanden SY, Qiao X, Neefjes J. New insights into the activities and toxicities of the old anticancer drug doxorubicin. The FEBS Journal. 2021; 288: 6095–6111.

[3] Sheibani M, Azizi Y, Shayan M, Nezamoleslami S, Eslami F, Farjoo MH, *et al*. Doxorubicin-Induced Cardiotoxicity: An Overview on Pre-clinical Therapeutic Approaches. Cardiovascular Toxicology. 2022; 22: 292–310.

[4] Fan HY, Wang XK, Li X, Ji K, Du SH, Liu Y, *et al*. Curcumin, as a pleiotropic agent, improves doxorubicin-induced nephrotic syndrome in rats. Journal of Ethnopharmacology. 2020; 250: 112502.

[5] Bohnert BN, Dörffel T, Daiminger S, Calaminus C, Aidone S, Falkenau A, *et al*. Retrobulbar Sinus Injection of Doxorubicin is More Efficient Than Lateral Tail Vein Injection at Inducing Experimental Nephrotic Syndrome in Mice: A Pilot Study. Laboratory Animals. 2019; 53: 564–576.

[6] Xiao M, Bohnert BN, Grahammer F, Artunc F. Rodent models to study sodium retention in experimental nephrotic syndrome. Acta Physiologica. 2022; 235: e13844.

[7] Zhang Q, Wu G, Guo S, Liu Y, Liu Z. Effects of tristetraprolin on doxorubicin (adriamycin)-induced experimental kidney injury through inhibiting IL-13/STAT6 signal pathway. American Journal of Translational Research. 2020; 12: 1203–1221.

[8] Feng R, Yuan X, Shao C, Ding H, Liebe R, Weng HL. Are we any closer to treating liver fibrosis (and if no, why not)? Journal of Digestive Diseases. 2018; 19: 118–126.

[9] Jing L, Su S, Zhang D, Li Z, Lu D, Ge R. Srolo Bzhtang, a traditional Tibetan medicine formula, inhibits cigarette smoke induced airway inflammation and muc5ac hypersecretion via suppressing IL-13/STAT6 signaling pathway in rats. Journal of Ethnopharmacology. 2019; 235: 424–434.

[10] Mitamura Y, Nunomura S, Nanri Y, Arima K, Yoshihara T, Komiya K, *et al*. Hierarchical control of interleukin 13 (IL-13) signals in lung fibroblasts by STAT6 and SOX11. The Journal of Biological Chemistry. 2018; 293: 14646–14658.

[11] Olsan EE, West JD, Torres JA, Doerr N, Weimbs T. Identification of targets of IL-13 and STAT6 signaling in polycystic kidney disease. American Journal of Physiology. Renal Physiology. 2018; 315: F86–F96.

[12] Liang Y, Yi P, Yuan DMK, Jie Z, Kwota Z, Soong L, *et al*. IL-33 induces immunosuppressive neutrophils via a type 2 innate lymphoid cell/IL-13/STAT6 axis and protects the liver against injury in LCMV infection-induced viral hepatitis. Cellular & Molecular Immunology. 2019; 16: 126–137.

[13] Sahebkar A, Kiaie N, Gorabi AM, Mannarino MR, Bianconi V, Jamialahmadi T, *et al*. A comprehensive review on the lipid and pleiotropic effects of pitavastatin. Progress in Lipid Research. 2021; 84: 101127.

[14] Elbaset MA, Mohamed BMSA, Hessin A, Abd El-Rahman SS, Esatbeyoglu T, Afifi SM, *et al*. Nrf2/HO-1, NF-κB and PI3K/Akt signalling pathways decipher the therapeutic mechanism of pitavastatin in early phase liver fibrosis in rats. Journal of Cellular and Molecular Medicine. 2024; 28: e18116.

[15] Elbaset MA, Mohamed BMSA, Moustafa PE, Esatbeyoglu T, Afifi SM, Hessin AF, *et al*. Renoprotective Effect of Pitavastatin against TAA-Induced Renal Injury: Involvement of the miR-93/PTEN/AKT/mTOR Pathway. Advances in Pharmacological and Pharmaceutical Sciences. 2024; 2024: 6681873.

[16] Vital KD, Cardoso BG, Lima IP, Campos AB, Teixeira BF, Pires LO, *et al*. Therapeutic effects and the impact of statins in the prevention of ulcerative colitis in preclinical models: A systematic review. Fundamental & Clinical Pharmacology. 2023; 37: 493–507.

[17] You HY, Zhang WJ, Xie XM, Zheng ZH, Zhu HL, Jiang FZ. Pitavastatin suppressed liver cancer cells in vitro and in vivo. OncoTargets and Therapy. 2016; 9: 5383–5388.

[18] Cheng BF, Gao YX, Lian JJ, Guo DD, Liu TT, Xie YF, *et al*. Anti-inflammatory effects of pitavastatin in interleukin-1β-induced SW982 human synovial cells. International Immunopharmacology. 2017; 50: 224–229.

[19] Ni M, Qin B, Xie L, Zhang X, Yang J, Lv H, *et al*. IL-13 Contributes to Drug Resistance of NK/T-Cell Lymphoma Cells by Regulating ABCC4. BioMed Research International. 2018; 2018: 2606834.

[20] Long L, Xiang H, Liu J, Zhang Z, Sun L. ZEB1 mediates doxorubicin (Dox) resistance and mesenchymal characteristics of hepatocarcinoma cells. Experimental and Molecular Pathology. 2019; 106: 116–122.

[21] Zhang Y, Li C, Zhang M, Li Z. IL-13 and IL-13Rα1 are overexpressed in extranodal natural killer/T cell lymphoma and mediate tumor cell proliferation. Biochemical and Biophysical Research Communications. 2018; 503: 2715–2720.

[22] Qin Y, Jiang Y, Sheikh AS, Shen S, Liu J, Jiang D. Interleukin-13 stimulates MUC5AC expression via a STAT6-TMEM16A-ERK1/2 pathway in human airway epithelial cells. International Immunopharmacology. 2016; 40: 106–114.

[23] Wu Q, Li W, Zhao J, Sun W, Yang Q, Chen C, *et al*. Apigenin ameliorates doxorubicin-induced renal injury via inhibition of oxidative stress and inflammation. Biomedicine & Pharmacotherapy. 2021; 137: 111308.

[24] Asaad GF, Hassan A, Mostafa RE. Anti-oxidant impact of Lisinopril and Enalapril against acute kidney injury induced by doxorubicin in male Wistar rats: involvement of kidney injury molecule-1. Heliyon. 2021; 7: e05985.

[25] Bilgic S, Armagan I. Effects of misoprostol treatment on doxorubicin induced renal injury in rats. Biotechnic & Histochemistry. 2020; 95: 113–120.

[26] Prado DS, Damasceno LEA, Sonego AB, Rosa MH, Martins TV, Fonseca MDM, *et al*. Pitavastatin ameliorates autoimmune neuroinflammation by regulating the Treg/Th17 cell balance through inhibition of mevalonate metabolism. International Immunopharmacology. 2021; 91: 107278.

[27] Li M, Liu X. Pitavastatin maintains MAPK7 expression and alleviates angiotensin II-induced vascular endothelial cell inflammation and injury. Experimental and Therapeutic Medicine. 2022; 23: 132.

[28] Kobayashi N, Takeshima H, Fukushima H, Koguchi W, Mamada Y, Hirata H, *et al*. Cardioprotective effects of pitavastatin on cardiac performance and remodeling in failing rat hearts. American Journal of Hypertension. 2009; 22: 176–182.

[29] Lahoti TS, Patel D, Thekkemadom V, Beckett R, Ray SD. Doxorubicin-induced in vivo nephrotoxicity involves oxidative stress-mediated multiple pro- and anti-apoptotic signaling pathways. Current Neurovascular Research. 2012; 9: 282–295.

[30] Owumi SE, Lewu DO, Arunsi UO, Oyelere AK. Luteolin attenuates doxorubicin-induced derangements of liver and kidney by reducing oxidative and inflammatory stress to suppress apoptosis. Human & Experimental Toxicology. 2021; 40: 1656–1672.

[31] AlAsmari AF, Ali N, Alharbi M, Alqahtani F, Alasmari F, Almoqbel D, *et al*. Geraniol Ameliorates Doxorubicin-Mediated Kidney Injury through Alteration of Antioxidant Status, Inflammation, and Apoptosis: Potential Roles of NF-κB and Nrf2/Ho-1. Nutrients. 2022; 14: 1620.

[32] Molehin OR, Adeyanju AA, Adefegha SA, Oyeyemi AO, Idowu KA. Protective mechanisms of protocatechuic acid against doxorubicin-induced nephrotoxicity in rat model. Journal of Basic and Clinical Physiology and Pharmacology. 2019; 30: 20180191.